J Radioanal Nucl Chem (2013) 295:335–343
DOI 10.1007/s10967-012-1860-5

Preliminary studies of ^{99m}Tc-PQQ-NMDAR binding and effect of specificity binding by mannitol

Xingqin Zhou · Yanyan Kong · Guoxian Cao · Jiankang Zhang

Received: 17 March 2012 / Published online: 3 June 2012

Abstract Pyrroloquinoline quinone (PQQ) is a powerful neuroprotectant that specifically binds to brain NMDA receptors and inhibits excitotoxicity. Imaging this binding reaction in the brain remains a long sought goal in this field of study, and one of the primary challenges remaining is enabling soluble labeled PQQ to pass the blood–brain barrier (BBB). Previously, our group successfully labeled PQQ with Technetium-99m (^{99m}Tc), a metastable nuclear isomer used in radioactive isotope medical tests. In this work, we determined the specific binding of ^{99m}Tc-PQQ and NMDAR by radioligand receptor assay. Ebselen (EB) and MK-801 both effectively inhibited ^{99m}Tc-PQQ binding. We then investigated methods of opening the BBB using mannitol to enable entry to the brain by ^{99m}Tc-PQQ. Our results showed that 7.5 mL/kg of 20 % mannitol effectively opened the BBB and 20 min was the optimum treatment time. Competition studies showed that mannitol did not affect the specific binding between ^{99m}Tc-PQQ and NMDA receptors. Using this method, the amount of ^{99m}Tc-PQQ uptake and retention was increased most significantly in the hippocampus and cortex, and re-opening the BBB did not affect binding. Together, our results demonstrate that the use of mannitol to open the BBB may contribute significantly to improving image quality by increasing the uptake amount of a water-soluble agent in brain.

Keywords NMDAR · ^{99m}Tc-PQQ · Radio-ligand receptor binding assay · Brain imaging · Blood–brain barrier

X. Zhou (✉) · Y. Kong · G. Cao · J. Zhang
Key Laboratory of Nuclear Medicine, Ministry of Health, Jiangsu Key Laboratory of Molecular Nuclear Medicine, Jiangsu Institute of Nuclear Medicine, Wuxi 214063, Jiangsu, China
e-mail: zhouxingqin@jsinm.org

Introduction

Pyrroloquinoline quinone (PQQ) is a ubiquitous molecule that is found in locations that vary from interstellar dust to human tissues. It is water soluble, heat stable, and capable of undergoing continuous redox cycling at a level at least 25 times greater than that of many other redox agents. PQQ is a redox cofactor in bacteria and is found in plant and animal tissues [1–4]. As an electron donor or *N*-methyl D-aspartate receptor (NMDAR) redox reaction site, PQQ readily reacts with nucleophiles to form stable condensation products [5]. PQQ's benefits as an antioxidant are so numerous that it has been considered for classification as a vitamin. PQQ's activity inhibits β-amyloid (1–42) fibril formation, the cytotoxic effects of solubleβ-amyloid (1–42) and fibrillation of mouse prion protein. It also protects against oxidative damage to the brain and protects other organs from external sources such as poisons or drugs [6].

In the brain, NMDAR is considered to be among the most critical molecular regulators of cognition, memory, motor control and synaptic plasticity. These receptors contain a "redox modulatory site" that strongly regulates receptor function. NMDARs are a type of receptor for the neurotransmitter glutamate, which is the primary excitatory neurotransmitter in the brain. Glutamate is found in 100 % of pyramidal neurons, approximately 60 % of total brain neurons, and accounts for virtually all cortico-cortical neurotransmission. Disturbances in NMDAR-mediated glutamatergic neurotransmission in the brain, primarily related to excitotoxicity, are present in many neurological and psychiatric disorders including epilepsy, Alzheimer's disease (AD) and schizophrenia [7–11]. It has been shown that PQQ interacts with the NMDAR redox site to inhibit glutamate-induced

cytotoxicity and produce beneficial physiological and cognitive outcomes.

Understanding the function of NMDAR in brain continues to be limited by a lack of effective imaging methods in vivo. Currently, positron emission tomography (PET) and single photon emission computed tomography (SPECT) are favored methods of imaging the living brain, and it is believed that developing a broad battery of radioligands specific for NMDA receptors would contribute to our knowledge regarding the density, spacial distribution, and function of these receptors in brain [12]. Unfortunately, many radio-probes are not ideal and ultimately are limited by their low fat solubility and consequent high non-specific binding. There is an urgent need to develop improved probes that can show distinct changes in NMDA receptors over the course of neurological disorders.

Technetium-99m (^{99m}Tc) is the most popular SPECT radioisotope. It is used in up to 85 % of diagnostic nuclear medical procedures every year [13, 14].

^{99m}Tc-PQQ was previously prepared in our laboratory and found to potentially accumulate predominantly in the hippocampus and cortex, which have a high density of NMDAR [15]. However, ^{99m}Tc-PQQ is water-soluble and negatively charged and has chelating groups that further limit its ability to pass through the blood–brain barrier (BBB). Therefore, in our previous work, image reconstruction was restricted because hardly any ^{99m}Tc-PQQ entered the brain and even less bound with NMDARs. Our next research goal became to improve the ability of ^{99m}Tc-PQQ to pass through the BBB.

The BBB forms a physical blockade to exclude from the brain nearly all neurotherapeutics and small molecule drugs [16]. The end result is a bottleneck in brain drug development, and this is the single most important factor limiting the future growth of neurotherapeutics. Hyperosmotic opening of the BBB has been developed as a tool to reversibly disrupt the BBB during administration of chemotherapeutic drugs, allowing for access to hidden marginal tumor cells and better clinical outcomes [17]. Mannitol has been used clinically to open the BBB for the delivery of some agents into the brain tissue [18].

In this work, the specificity binding of ^{99m}Tc-PQQ to NMDAR was investigated by Radio-ligand receptor binding assay (RRA). Regional distribution of ^{99m}Tc-PQQ in brain was tested and the effect of the mannitol dose on BBB opening was studied. Moreover, whether BBB opening affect the specificity binding of ^{99m}Tc-PQQ to NMDA receptor were further studied. This provides a new method for improving the uptake of water-soluble imaging reagent in brain.

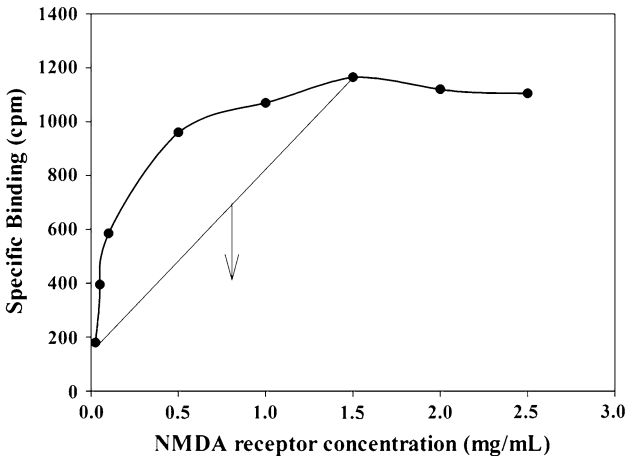

Fig. 1 Specific binding of ^{99m}Tc-PQQ to NMDAR at various concentrations

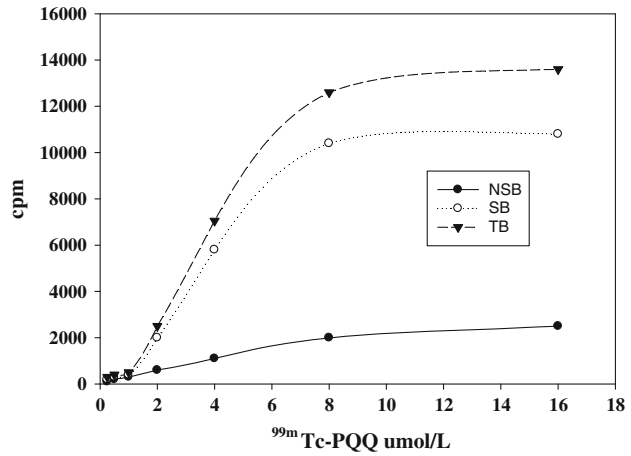

Fig. 2 Saturation curve of ^{99m}Tc-PQQ to NMDA receptor

Experimental procedures

Materials and reagents

PQQ was obtained from ShanghaiMed Co. (China). SnF_2 anhydrous, MK801, and Ebselen (EB) were purchased from Sigma-Aldrich (USA). All the other analytical chemical reagents employed were purchased from commercial sources and used without further purification. $Na^{99m}TcO_4$ pertechnetate obtained from locally produced fission based ^{99}Mo/^{99m}Tc generator system (Chengdu Nuclear Isotope Qualcomm Inc., China) was used for radio labeling.

Animals

Sprague–Dawley (SD) rats were supplied by Jiangsu Institute of Nuclear Co., Ltd. (China). The NMDA receptor was prepared from SD rats. Mice (ICR) were purchased

from Shanghai SLAC Laboratory Animal Center (Shanghai, China). ICR mice (20 ± 1 g) were divided randomly into six groups with three mice per group experiments for the opening BBB experiments by mannitol. The animal experiment in this study was approved by the Animal Care and Ethics Committee of Jiangsu Institute of Nuclear Medicine.

Preparation of ^{99m}Tc-PQQ

^{99m}Tc-PQQ was prepared as described previously [15]. Briefly, 0.05 mL EDTA-2Na (10 mg/mL) and 0.15 mL PQQ (6.6 mg/mL) were added to a 1.5-mL centrifuge tube, followed by 0.1 mL Na[^{99m}Tc]O_4 (40 MBq) and then immediately by 0.03 mL freshly prepared SnF_2 solution(1 mg/mL in 0.1 M HCl). The volume was adjusted to 1 mL using phosphate buffer (pH 6.0). The mixture was reacted at room temperature for 30 min. ^{99m}Tc-PQQ was purified by radio-HPLC to obtain high specific activity. Radiochemical purity (RCP) was tested by thin-layer chromatography (TLC) using acetone as the mobile phase.

RRA

Sources of NMDAR

NMDAR was extracted from SD rats as previously described [19]. Brains (removed midbrain, cerebellum, and spinal cord) were homogenized sufficiently by glass homogenizer in 10 volumes of buffer B (10 mM HEPES buffer which contented 1 mM EDTA). Then the homogenates were centrifuged at 2,400 r/min for 10 min at 4 °C to remove impurities. The remained supernatant was centrifuged for 20 min. The precipitants were resuspended in buffer B and centrifuged again. This procedure was repeated at least three times. Then the pellet was resuspended in buffer A (10 mM HEPES) in the original volume. The homogenates were then incubated at 37 °C for 30 min, followed by three additional centrifugation steps in buffer A. The entire operation was completed in an ice bath. The pellet was resuspended in buffer A in the original volume and stored in 1-mL aliquots at −20 °C until use. The protein content was determined by Coomassie Brilliant Blue Method.

The effects of NMDAR concentration and incubation time on specific binding

NMDAR was diluted to 0.025, 0.05, 0.1, 0.5, 1, 1.5, 2, and 2.5 mg/mL with buffer A. Samples were divided into three groups: total binding (TB), nonspecific binding (NSB) and blank (BLANK). TB was tested with 0.3 mL of each protein concentration. For each tube, 0.1 mL buffer C (5 % Tween-20 in buffer A) and 0.1 mL ^{99m}Tc-PQQ (1.0 μmol/L) were added, and buffer C was used to adjust the volume to 0.6 mL. NSB was tested using the same procedure, except that 0.1 mL PQQ (200 μmol/L) was added to the tube. The blank was assayed with only 0.1 mL ^{99m}Tc-PQQ and 0.5 mL buffer C. All the tubes were incubated at 37 °C for 30 min in a water bath and placed on ice for 5 min to stop the reaction. GF/B glass fiber filter paper was used for filtering with 5 % bovine serum albumin (BSA). The ZT2-type long-cell collector was used for filtration. The products were washed with 4 mL buffer C three times before removing the membranes to count the samples using γ-counter. The incubation time experiment was done in the same way, using 0.5 mg/mL protein in each tube and incubating the samples for 5, 10, 20, 30, 40, 50, or 60 min, followed by leaching and counting.

The effect of different socking mediums (including PEI, Tris-HCl, BSA, serum and saline), rinse time and amount on the impact of specific binding on NMDA receptor were studied as above described.

Determining equilibrium dissociation constant K_d

The same steps described in the above section were used with 0.1 mL ^{99m}Tc-PQQ at 0.025, 0.5, 1, 2, 4, 8, or 16 μmol/L added. The samples were stirred, incubated at 37 °C for 30 min, leached, and counted. The equilibrium dissociation constant K_d was estimated according to a saturation curve.

Competition binding assay

The three antagonists, EB (+)-MK-801, and halperidol were used for experiments following same steps described above with 0.1 mL ^{99m}Tc-PQQ (1 μmol/L) and the antagonists at 1×10^{-3}, 1×10^{-4}, 1×10^{-5}, 1×10^{-6}, 1×10^{-7}, 1×10^{-8}, 1×10^{-9}, 1×10^{-10}, 1×10^{-11}, or 1×10^{-12} mol/L in each tube.

Opening the BBB

The dosage of mannitol

ICR mice were divided randomly into six groups with three animals weighing 20 ± 1 g per group. For BBB studies, different concentrations of 20 % mannitol (0.25, 2.5, 5, 7.5, 10, and 15 mL/kg) were injected 5 min prior to ^{99m}Tc-PQQ injection (7.4 MBq, 0.2 mL). The animals were sacrificed 5 min after injection of ^{99m}Tc-PQQ. The brain

was rapidly removed, chilled and dissected. Samples from different brain regions (striatum [ST], hippocampus [HP], cerebellum [CB], thalamus [TH], brain stem [BS], frontal lobe [FT], parietal lobe [PT], temporal lobe [TR], and occipital lobe [OT]) were collected, weighed and counted. The percentage of injected dose per gram (%ID/g) was calculated by comparing its activating with appropriate standard of injected dose (ID).

Mannitol incubation time

ICR mice (20 ± 1 g) were divided into six groups with three mice per group experiments to determine the incubation time for opening the BBB. ^{99m}Tc-PQQ (RCP > 95 %,7.4 MBq, 0.2 mL) was injected via the tail vein after giving 20 % mannitol for 1, 15, 30, 60, 240, and 360 min, and the mice were sacrificed 5 min after injection of ^{99m}Tc-PQQ. Regional brain distribution was determined as described above.

Confirmation of optimized conditions

The brain biodistribution experiment in the presence of 20 % mannitol (7.5 mL/kg) with 0.9 % saline was as control group. Twenty minutes after the first injection of 20 % mannitol (control by 0.9 % saline), ^{99m}Tc-PQQ was injected (7.4 MBq, 0.2 mL). Mice in the two groups were sacrificed at 5, 15, 30, 60 180 or 360 min post-injection ($n = 3$). The average ratios and standard deviations of %ID/g tissue of the different brain regions relative to that in thalamus were calculated.

Reversible opening of the BBB

The effect of BBB opening on the specific binding of ^{99m}Tc-PQQ was studied using ICR mice by control (mannitol) and experiment (mannitol + EB) treatment. Twenty minutes after the first injection of 20 % mannitol (7.5 mL/kg), ^{99m}Tc-PQQ was injected (7.4 MBq, 0.2 mL) in the control group. EB (51.4 mg/kg) was also injected in the experiment group. Mice in the two groups were sacrificed 5, 30 or 60 min post-injection ($n = 3$). The ratios of the values in different brain regions to the value in thalamus were calculated.

Data analysis

The average count of the blank samples was subtracted from the average count of the TB and NSB samples, and SB (specific binding) = TB − NSB. B_{max} and K_d were calculated by using software written according to the Clarlc occupancy theory of zone B.

Results

NMDAR and radioligand preparation

For in vitro experiments, NMDAR was extracted from SD rats as described by Reynolds and Sharma [19]. Concentration was determined to be approximately 3.876 mg/mL. ^{99m}Tc-PQQ was prepared to a radiochemical purity of greater than 95 % according to the method of Kong et al. [15]. Its specific activity was 2.2×10^{13} Bq/g. The results of paper electrophoresis indicated that the complex has a negative charge. ^{99m}Tc-PQQ is water soluble due to its hydrophilic side group (lgP = −1.49).

Determination of specific binding

Our first goal was to establish and optimize the signal for specific binding between ^{99m}Tc-PQQ and NMDAR using RRA. A known concentration of radioligand (1 μmol/L) corresponding to approximately 625 counts per minute (cpm) was incubated with varied concentrations of NMDAR protein in order to determine total binding (TB). A parallel experiment to determine non-specific binding (NSB) was completed that included the addition of 200-fold excess of unlabeled PQQ to the binding reaction. This ensured that all the NMDAR sites would be occupied by unlabeled PQQ and the measured radio-activity would be the non-specific binding. Specific binding (SB) was calculated from the difference between TB and NSB. Data points were fit to a spline curve and the optimal NMDAR concentration was determined to be 0.8 mg/mL ($C_{NMDAR} = [C_{starting\ point} + C_{highest\ point}]/2$) (Fig. 1).

^{99m}Tc-PQQ saturation curve

We determined maximum binding capacity B_{max} and the equilibrium dissociation constant K_d from the ^{99m}Tc-PQQ saturation curve (Fig. 2). NMDAR was incubated with varied concentrations of ^{99m}Tc-PQQ, and the data points were fit to a spline curve. B_{max} was determined to be 6.648 μmol/L ($n = 3$) and K_d 2.381 nmol/mg.

Competition curves

To confirm that the binding in our reactions was legitimate and comparable to PQQ-NMDAR binding behavior in actual cells, we conducted competitive binding experiments using Ebselen (EB). Ebselen is demonstrated to have neuroprotective effects in clinical trials and has been shown to bind the NMDAR redox modulatory site. We first determined the % Bound for ^{99m}Tc-PQQ in the presence of varied amounts of EB. From plotting % Bound as a function of the log[EB], we obtained the half maximal

inhibitory concentration (IC_{50}) of EB, which was 1.968 nmol/L. We then were able to calculate the equilibrium dissociation constant for EB (K_i), which was 1.919 nmol/L. This value indicates a slightly higher affinity for EB-NMDAR binding than for ^{99m}Tc-PQQ-NMDAR binding, and the data show a clear inhibitory effect by EB. Together, these results suggest that the radiolabeled ligand binds NMDAR in a manner that is comparable to binding behavior in live cells.

We also used an uncompetitive NMDAR antagonist, MK-801 in competition studies. MK-801 has been shown to bind NMDAR in the ion channel as a means of blocking receptor activity. The NMDAR redox modulatory site exerts effects on the activity of MK-801, and we investigated whether the reverse effects also applied to our system. Using the method just described, we found this to be the case in spite of the fact that MK-801 has an IC_{50} of 11.220 nmol/L and a K_i of 10.940 nmol/L. High values of IC_{50} and K_i suggest that MK-801 would not inhibit ^{99m}Tc-PQQ-NMDAR binding, but the inhibitory effects were seen in our results which suggested that some indirect mechanism maybe play a some role. As a control, we used haloperidol, a dopamine D_2 receptor and σ receptor antagonist. It had no effect on ^{99m}Tc-PQQ-NMDAR binding. As a control, we used haloperidol, a dopamine D_2 receptor and σ receptor antagonist. It had no effect on ^{99m}Tc-PQQ-NMDAR binding (Fig. 3).

In vivo studies

The effect of mannitol concentration on opening the BBB

The studies of cerebral receptor imaging agents were generally from in vitro to in vivo, and include affinity, uptake in brain and other properties. In this work, opening BBB in vivo to improve the uptake in brain was performed using mannitol. Six parallel experiments were conducted using three ICR mice in each. Varied concentrations of 20 % mannitol were administered to the mice 5 min prior to ^{99m}Tc-PQQ injection. Saline was used as a control. Animals were sacrificed 5 min after injection of ^{99m}Tc-PQQ, and the brains were analyzed by comprehensive dissection. The effect of dose on the uptake of ^{99m}Tc-PQQ in brain is shown in Fig. 4, and the results for spacial distribution in several regions of the brain are summarized in Table 1. Thalamus (TH) has a lower distribution than other regions and is considered the "reference region." Ratios of other brain regions compared to TH provide information on the relative abundance of NMDAR in different parts of the brain. To avoid damaging brain tissue with high doses of mannitol, 7.5 mL/kg 20 % mannitol was selected as the optimum dose in subsequent experi ments. This concentration produced a percentage dose of approximately 0.4 %ID/g (Fig. 4).

The effect of mannitol incubation time on opening the BBB

Next, we determined the best mannitol incubation time. Six parallel experiments were conducted in which mice were treated with 7.5 mL/kg 20 % mannitol for different time durations. This was followed by ^{99m}Tc-PQQ treatment for 5 min, animal sacrifice, and comprehensive dissection. Maximum ^{99m}Tc-PQQ uptake occurred in the 30 min mannitol treatment group (See Table 2 and Fig. 5).

Spacial distribution of ^{99m}Tc-PQQ uptake in brain

Using the optimized treatment parameters, we determined that the spacial distribution of ^{99m}Tc-PQQ in brain has the highest density in the HP and FT, as indicated by the HP/

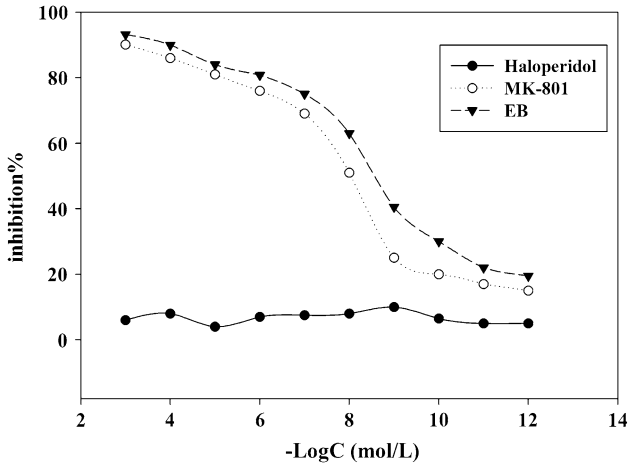

Fig. 3 Competition curves of EB and MK-801

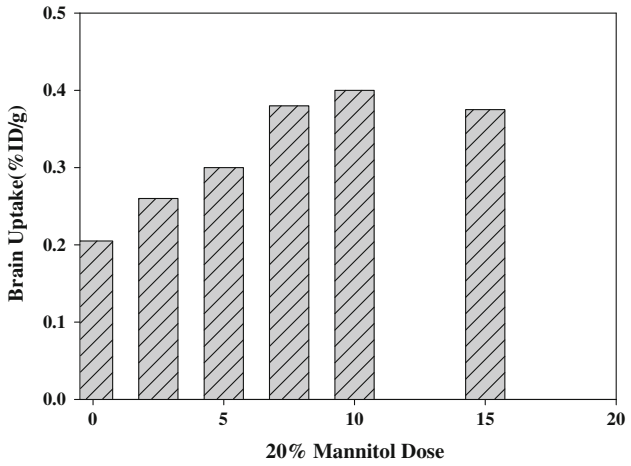

Fig. 4 The effect of mannitol dose on the brain uptake of ^{99m}Tc-PQQ

Table 1 The effect of mannitol dose on the distribution of ^{99m}Tc-PQQ in brain

	Mannitol (mL/kg)					
	0.25	2.5	5	7.5	10	15
Region						
Striatum	0.155 ± 0.046	0.230 ± 0.072	0.196 ± 0.030	0.221 ± 0.038	0.222 ± 0.043	0.177 ± 0.035
Hippocampus	0.211 ± 0.044	0.264 ± 0.052	0.306 ± 0.056	0.371 ± 0.003	0.346 ± 0.028	0.341 ± 0.046
Thalamus	0.166 ± 0.056	0.174 ± 0.005	0.172 ± 0.064	0.194 ± 0.049	0.168 ± 0.012	0.164 ± 0.042
Cerebellum	0.165 ± 0.047	0.214 ± 0.049	0.213 ± 0.021	0.225 ± 0.034	0.207 ± 0.016	0.225 ± 0.031
Brain stem	0.178 ± 0.048	0.251 ± 0.040	0.254 ± 0.028	0.268 ± 0.006	0.300 ± 0.067	0.274 ± 0.048
Frontal lobe	0.305 ± 0.040	0.374 ± 0.097	0.453 ± 0.076	0.518 ± 0.006	0.536 ± 0.072	0.489 ± 0.061
Parietal lobe	0.315 ± 0.048	0.338 ± 0.090	0.389 ± 0.075	0.491 ± 0.040	0.504 ± 0.056	0.473 ± 0.035
Temporal lobe	0.262 ± 0.013	0.280 ± 0.077	0.305 ± 0.040	0.401 ± 0.046	0.409 ± 0.037	0.371 ± 0.076
Occipital lobe	0.266 ± 0.024	0.255 ± 0.029	0.264 ± 0.054	0.371 ± 0.034	0.419 ± 0.051	0.373 ± 0.068
Ratio to thalamus value						
HP/TH	1.306 ± 0.151	1.512 ± 0.262	1.906 ± 0.510	2.019 ± 0.606	2.066 ± 0.148	2.229 ± 0.890
FT/TH	1.940 ± 0.514	2.142 ± 0.511	2.218 ± 0.311	2.815 ± 0.849	3.190 ± 0.293	3.130 ± 0.944
PT/TH	1.988 ± 0.501	1.935 ± 0.479	2.472 ± 0.871	2.039 ± 0.138	3.002 ± 0.190	2.983 ± 0.606
TR/TH	1.681 ± 0.446	1.602 ± 0.419	1.957 ± 0.733	2.205 ± 0.820	2.440 ± 0.087	2.311 ± 0.466
OT/TH	1.692 ± 0.402	1.468 ± 0.195	1.691 ± 0.653	2.041 ± 0.763	2.495 ± 0.128	2.357 ± 0.607

Table 2 The distribution of ^{99m}Tc-PQQ in brain at different time points after mannitol injection

	Time after mannitol injection (min)					
	1	15	30	60	240	360
Region						
Striatum	0.224 ± 0.045	0.459 ± 0.080	0.386 ± 0.053	0.152 ± 0.015	0.086 ± 0.014	0.051 ± 0.010
Hippocampus	0.361 ± 0.051	0.674 ± 0.091	0.753 ± 0.165	0.331 ± 0.081	0.197 ± 0.023	0.118 ± 0.013
Thalamus	0.203 ± 0.034	0.325 ± 0.032	0.430 ± 0.109	0.141 ± 0.011	0.091 ± 0.009	0.045 ± 0.008
Cerebellum	0.240 ± 0.024	0.483 ± 0.034	0.534 ± 0.100	0.187 ± 0.024	0.104 ± 0.004	0.058 ± 0.008
Brain stem	0.342 ± 0.054	0.531 ± 0.026	0.614 ± 0.101	0.215 ± 0.030	0.133 ± 0.010	0.065 ± 0.003
Frontal lobe	0.521 ± 0.066	0.927 ± 0.113	1.146 ± 0.106	0.366 ± 0.028	0.296 ± 0.019	0.155 ± 0.022
Parietal lobe	0.533 ± 0.104	0.860 ± 0.123	1.017 ± 0.056	0.358 ± 0.040	0.283 ± 0.021	0.137 ± 0.027
Temporal lobe	0.450 ± 0.125	0.667 ± 0.143	0.842 ± 0.056	0.298 ± 0.022	0.242 ± 0.027	0.108 ± 0.009
Occipital lobe	0.496 ± 0.152	0.767 ± 0.099	0.925 ± 0.058	0.362 ± 0.067	0.270 ± 0.034	0.136 ± 0.025
Ratio to thalamus value						
HP/TH	1.784 ± 0.107	2.082 ± 0.267	1.801 ± 0.515	2.326 ± 0.396	2.190 ± 0.436	2.666 ± 0.267
FT/TH	2.582 ± 0.271	2.880 ± 0.525	2.750 ± 0.533	2.608 ± 0.352	3.274 ± 0.387	3.508 ± 0.388
PT/TH	2.679 ± 0.730	2.668 ± 0.499	2.458 ± 0.560	2.547 ± 0.405	3.114 ± 0.090	3.082 ± 0.321
TR/TH	2.260 ± 0.758	2.093 ± 0.649	2.042 ± 0.525	2.112 ± 0.165	2.669 ± 0.350	2.463 ± 0.463
OT/TH	2.520 ± 0.973	2.393 ± 0.525	2.238 ± 0.539	2.569 ± 0.535	2.973 ± 0.345	3.031 ± 0.132

TH and FT/TH ratios in Table 3, particularly for the 5, 30 and 60 min time points. This result is in agreement with our previous findings. We conducted competition studies using EB and found that in vivo, as in our in vitro experiments, EB inhibited ^{99m}Tc-PQQ-NMDAR binding in the presence of mannitol.

Reversible opening of the BBB on the specific binding of ^{99m}Tc-PQQ to NMDAR

To further confirm that mannitol does not affect the binding specificity of ^{99m}Tc-PQQ to NMDAR, we examined the distribution of ^{99m}Tc-PQQ upon closing the BBB with EB.

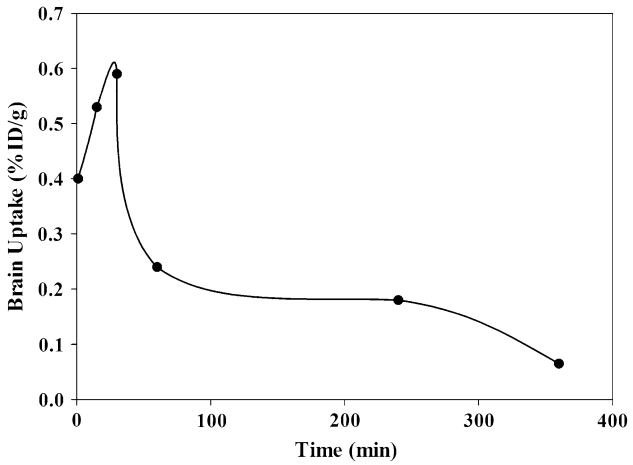

Fig. 5 The effect of mannitol on the time to BBB opening

As shown in Fig. 6, the HP/TH and FT/TH ratios in the presence of mannitol and EB were significantly lower than the group that received mannitol only. From our results, it is clear that mannitol does not affect the binding specificity of ^{99m}Tc-PQQ to NMDAR.

Discussion

Hyperosmolar mannitol has been used clinically to open the BBB for the administration of pharmacological agents to the brain tissue [18]. In addition, Brown also indicated that mannitol-induced BBB disruption may allow improved design and/or enhancement of the penetration of chemotherapeutics and other types of drugs to better treat a multitude of neurological disorders [17]. Previously, our

Table 3 Uptake of ^{9m}Tc-PQQ in brain of mice with time after mannitol injection

	Time after mannitol injection (min)					
	5		15		30	
	Mannitol	Control	Mannitol	Control	Mannitol	Control
Region						
Striatum	0.464 ± 0.097*	0.141 ± 0.005	0.258 ± 0.037*	0.064 ± 0.004	0.177 ± 0.024*	0.072 ± 0.008
Hippocampus	0.723 ± 0.108*	0.186 ± 0.006	0.378 ± 0.052*	0.124 ± 0.017	0.329 ± 0.043*	0.073 ± 0.015
Thalamus	0.472 ± 0.037*	0.164 ± 0.028	0.236 ± 0.026	0.103 ± 0.025	0.210 ± 0.025**	0.111 ± 0.028
Cerebellum	0.517 ± 0.118	0.396 ± 0.097	0.283 ± 0.049	0.350 ± 0.309	0.218 ± 0.030	0.144 ± 0.044
Brain stem	0.538 ± 0.073**	0.348 ± 0.023	0.278 ± 0.022**	0.192 ± 0.045	0.266 ± 0.042	0.201 ± 0.072
Frontal lobe	0.963 ± 0.172*	0.278 ± 0.018	0.520 ± 0.044*	0.176 ± 0.091	0.464 ± 0.022*	0.141 ± 0.012
Parietal lobe	1.026 ± 0.210*	0.300 ± 0.043	0.489 ± 0.028*	0.150 ± 0.027	0.451 ± 0.044*	0.095 ± 0.002
Temporal lobe	0.762 ± 0.121*	0.280 ± 0.014	0.427 ± 0.041*	0.172 ± 0.019	0.392 ± 0.073*	0.125 ± 0.021
Occipital lobe	0.882 ± 0.206*	0.310 ± 0.033	0.450 ± 0.093*	0.155 ± 0.046	0.354 ± 0.055*	0.109 ± 0.033
Ratio to thalamus value						
HP/TH	1.531 ± 0.334	1.156 ± 0.170	1.601 ± 0.102	1.236 ± 0.259	1.564 ± 0.068*	0.661 ± 0.075
FT/TH	2.034 ± 0.260	1.721 ± 0.234	2.213 ± 0.133**	1.947 ± 0.098	2.231 ± 0.300	1.732 ± 0.209
PT/TH	2.163 ± 0.373	1.841 ± 0.141	2.125 ± 0.148**	1.478 ± 0.234	2.165 ± 0.325*	0.890 ± 0.200
TR/TH	1.608 ± 0.288	1.746 ± 0.338	1.816 ± 0.132	1.702 ± 0.271	1.859 ± 0.178*	1.141 ± 0.178
OT/TH	1.867 ± 0.371**	1.077 ± 0.057	1.906 ± 0.296**	1.233 ± 0.275	1.698 ± 0.302**	0.980 ± 0.200
	60		180		360	
	Mannitol	Control	Mannitol	Control	Mannitol	Control
Region						
Striatum	0.131 ± 0.004*	0.031 ± 0.005	0.055 ± 0.011**	0.023 ± 0.010	0.018 ± 0.003	0.016 ± 0.003
Hippocampus	0.204 ± 0.015*	0.041 ± 0.005	0.132 ± 0.053	0.064 ± 0.052	0.028 ± 0.007	0.033 ± 0.026
Thalamus	0.139 ± 0.019*	0.066 ± 0.009	0.085 ± 0.035**	0.029 ± 0.003	0.020 ± 0.003	0.024 ± 0.003
Cerebellum	0.142 ± 0.017	0.100 ± 0.008	0.077 ± 0.013	0.064 ± 0.018	0.026 ± 0.003	0.049 ± 0.010
Brain stem	0.144 ± 0.040	0.135 ± 0.033	0.073 ± 0.015**	0.041 ± 0.005	0.029 ± 0.003	0.042 ± 0.007
Frontal lobe	0.267 ± 0.008*	0.085 ± 0.026	0.187 ± 0.061**	0.028 ± 0.012	0.044 ± 0.011	0.030 ± 0.011
Parietal lobe	0.239 ± 0.006*	0.069 ± 0.003	0.152 ± 0.026*	0.040 ± 0.008	0.042 ± 0.009**	0.024 ± 0.003
Temporal lobe	0.228 ± 0.031*	0.072 ± 0.008	0.141 ± 0.036*	0.036 ± 0.003	0.030 ± 0.012	0.026 ± 0.003

Table 3 continued

	60		180		360	
	Mannitol	Control	Mannitol	Control	Mannitol	Control
Occipital lobe	0.232 ± 0.046*	0.058 ± 0.025	0.132 ± 0.092	0.043 ± 0.003	0.030 ± 0.005	0.031 ± 0.006
Ratio to thalamus value						
HP/TH	1.487 ± 0.234*	0.627 ± 0.060	1.599 ± 0.227*	0.710 ± 0.035	1.395 ± 0.167*	0.688 ± 0.115
FT/TH	1.935 ± 0.214**	1.265 ± 0.253	2.279 ± 0.480**	1.373 ± 0.096	2.161 ± 0.315**	1.391 ± 0.277
PT/TH	1.740 ± 0.258**	1.058 ± 0.113	1.932 ± 0.524	1.366 ± 0.145	2.081 ± 0.301*	1.098 ± 0.015
TR/TH	1.656 ± 0.296	1.116 ± 0.284	1.739 ± 0.298	1.256 ± 0.197	1.437 ± 0.369	1.093 ± 0.068
OT/TH	1.677 ± 0.349**	0.849 ± 0.296	1.428 ± 0.472	0.743 ± 0.021	1.482 ± 0.053*	0.710 ± 0.031

* $P < 0.01$ and ** $P < 0.05$ relative to control group

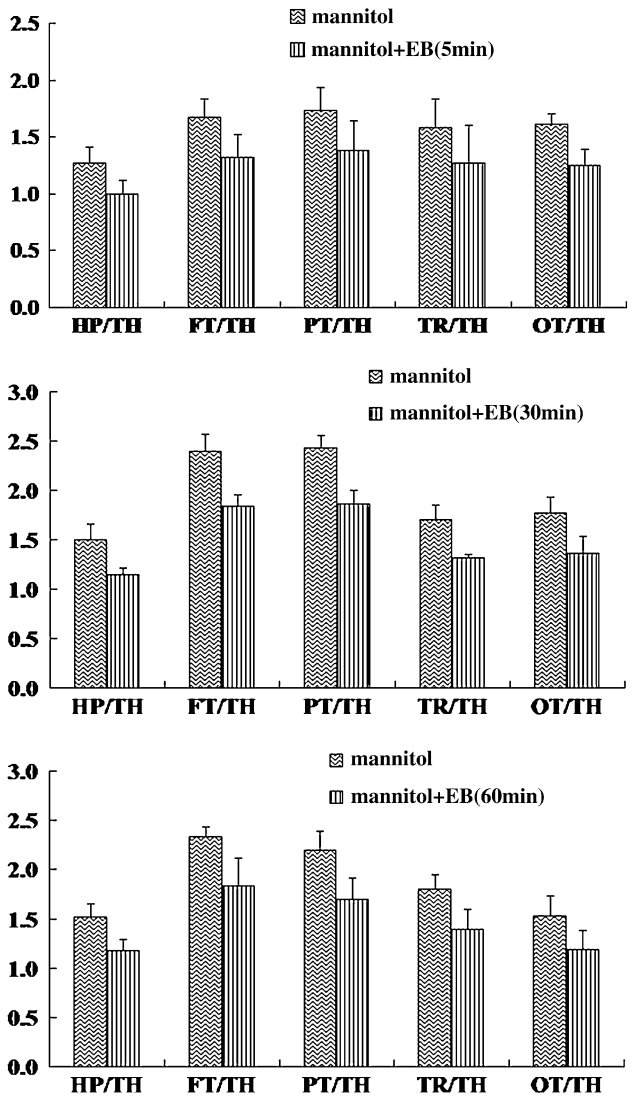

Fig. 6 The effects of mannitol on the binding specificity of ^{99m}Tc-PQQ

laboratory produced ^{99m}Tc-labeled PQQ. Biodistribution studies in mice showed that the activity of ^{99m}Tc-PQQ in brain reached its maximum by 5 min. Here we characterized the binding between ^{99m}Tc-PQQ and NMDAR in vitro and in vivo. Using RRAs, we determined ligand-receptor binding parameters including specific binding, maximum binding capacity and equilibrium constant. We established a method for opening the BBB using mannitol to enable entry of ^{99m}Tc-PQQ into the brain and mapped the regional distribution of the radioligand in brain. Specifically, our study shows that using mannitol to open the BBB significantly increased the levels of ^{99m}Tc-PQQ in brain. Target tissues with abundant NMDAR, such as the hippocampus and cortex, also increased uptake and retention of ^{99m}Tc-PQQ. Using competitive inhibition and reversible BBB opening experiments with EB, we have validated the binding between receptor and radioligand to be comparable to unlabeled PQQ and not affected by mannitol. Furthermore, our results strongly suggest that the BBB can be opened multiple times without affecting ^{99m}Tc-PQQ-NMDAR binding. The use of mannitol with ^{99m}Tc-PQQ should contribute significantly to improving image quality by increasing the uptake of a water-soluble agent in brain.

Acknowledgments This work was supported by the National Natural Science Foundation of China (30770602) and the Natural Science Foundation of Jiangsu Province, China (BK2010157, BK2011167).

References

1. Stites TE, Mitchell AE, Rucker RB (2000) Physiological importance of quinoenzymes and the O-quinone family of cofactors. J Nutr 130:719–727
2. McIntire WS (1998) Newly discovered redox cofactors: possible nutritional, medical, and pharmacological relevance to higher animals. Annu Rev Nutr 18:145–177
3. Davidson VL (2001) Pyrroloquinoline quinone (PQQ) from methanol dehydrogenase and tryptophan tryptophylquinone (TTQ) from methylamine dehydrogenase. Adv Protein Chem 58:95–140
4. Anthony C (2001) Pyrroloquinoline quinone (PQQ) and quinoprotein enzymes. Antioxid Redox Signal 3:757–774

5. Zhang P, Xu YP, Sun JX et al (2009) Protection of pyrroloquinoline quinone against methylmercury-induced neurotoxicity via reducing oxidative stress. Free Radical Res 43(3):224–233
6. Rucker R, Chowanadisai W, Nakano M (2009) Potential physiological importance of pyrroloquinoline quinone. Altern Med Rev 14(3):268–277
7. Ganapathy PS, White RE, Ha Y et al (2011) The role of *N*-methyl-D-aspartate receptor activation in homocysteine-induced death of retinal ganglion cells. Invest Ophthalmol Vis Sci 52(8):5515–5524
8. Ohnuma T, Arai H (2011) Significance of NMDA receptor-related glutamatergic amino acid levels in peripheral blood of patients with schizophrenia. Prog Neuropsychopharmacol Biol Psychiatry 35(1):29–39
9. Tsai GE, Lin PY (2010) Strategies to enhance *N*-methyl-D-aspartate receptor-mediated neurotransmission in schizophrenia, a critical review and meta-analysis. Curr Pharm Des 16(5): 522–537
10. Yang JH, Wada A, Yoshida K et al (2010) Brain-specific Phgdh deletion reveals a pivotal role for L-serine biosynthesis in controlling the level of D-serine, an *N*-methyl-D-aspartate receptor co-agonist, in adult brain. J Biol Chem 285(53):41380–41390
11. Frasca A, Aalbers M, Frigerio F et al (2011) Misplaced NMDA receptors in epileptogenesis contribute to excitotoxicity, neurobiology of disease. Neurobiol Dis 43(2):507–515
12. Sobrio F, Gilbert G, Perrio C et al (2010) PET and SPECT imaging of the NMDA receptor system: an overview of radiotracer development. Mini Rev Med Chem 10(9):870–886
13. Hansell C (2008) Nuclear medicine's double hazard. Nonprolif Rev 15:185–208
14. Eckelman WC (2009) Unparalleled contribution of technetium-99m to medicine over 5 decades. JACC Cardiovasc Imaging 2:364–368
15. Kong YY, Zhou XQ, Cao GX et al (2010) Preparation of ^{99m}Tc-PQQ and preliminary biological evaluation for the NMDA receptor. J Radioanal Nucl Chem 286(1):93–101
16. Pardridge WM (2005) The blood-brain barrier: bottleneck is brain drug development. J Am Soc Exp Neuro Ther 2:3–14
17. Brown RC, Egleton RD, Davis TP (2004) Mannitol opening of the blood–brain barrier: regional variation in the permeability of sucrose, but not 86Rb+ or albumin. Brain Res 1014:221–227
18. Chi OZ, Hunter C, Liu X et al (2008) Effects of VEGF on the blood-brain barrier disruption caused by hyperosmolarity. Pharmacology 82:187–192
19. Reynolds IJ, Sharma TA (1999) The use of ligand binding in assays of NMDA receptor function. Methods Mol Biol 128:93–102